## Defense Technical Information Center
## Compilation Part Notice

# ADP011173

TITLE: Active Control of Combustion Instabilities in Gas Turbine Engines
for Low Emissions. Part II: Adaptive Control Algorithm Development,
Demonstration and Performance Limitations

DISTRIBUTION: Approved for public release, distribution unlimited

This paper is part of the following report:

TITLE: Active Control Technology for Enhanced Performance Operational
Capabilities of Military Aircraft, Land Vehicles and Sea Vehicles
[Technologies des systemes a commandes actives pour l'amelioration des
performances operationnelles des aeronefs militaires, des vehicules
terrestres et des vehicules maritimes]

To order the complete compilation report, use: ADA395700

The component part is provided here to allow users access to individually authored sections
of proceedings, annals, symposia, etc. However, the component should be considered within
the context of the overall compilation report and not as a stand-alone technical report.

The following component part numbers comprise the compilation report:
ADP011101 thru ADP011178

# Active Control of Combustion Instabilities in Gas Turbine Engines for Low Emissions. Part II: Adaptive Control Algorithm Development, Demonstration and Performance Limitations

Andrzej Banaszuk
United Technologies Research Center,
MS129-15, 411 Silver Lane, East Hartford, CT 06108, USA
tel. 860 610 7381, **banasza@utrc.utc.com**

Youping Zhang
Numerical Technologies, Inc.
70 West Plumeria Drive San Jose, CA 95134-2134, USA
tel. 408 919 1910 ext 343 **yzhang@numeritech.com**

Clas A. Jacobson
United Technologies Research Center,
MS129-15, 411 Silver Lane, East Hartford, CT 06108, USA
tel. 860 610 7652, **jacobsca@utrc.utc.com**

## Abstract

We present results of experiment with two distinct extremum-seeking adaptive algorithms for control of combustion instability suitable for reduction of acoustic pressure oscillations in gas turbine over large range of operating conditions. The algorithms consists of a frequency tracking Extended Kalman Filter to determine the in-phase component, the quadrature component, and the magnitude of the acoustic mode of interest, and a phase shifting controller with the controller phase tuned using an extremum-seeking algorithms. The algorithms are also applicable for control of oscillations of systems whose oscillation frequency and optimal control phase shift depends on operating conditions, and which are driven by strong broad-band disturbance. The algorithms have been tested in combustion experiments involving full-scale engine hardware and during simulated fast engine transients.

## 1 Introduction

Emphasis on reducing the levels of pollutants created by industrial gas turbine combustors has led to the development of lean, premixed combustor designs, as premixing large amounts of air with the fuel prior to its injection into the combustor greatly reduces peak temperatures within the combustor and leads to lower NOx emissions. However, premixed combustors are often susceptible to thermoacoustic combustion instabilities, which can lead to large pressure oscillations in the combustor. These pressure oscillations result in increased noise and decreased durability. The goal of using active combustion instability control on a gas turbine engine is to keep pressure oscillations at an acceptable level over a large range of operating conditions.

Experiments and model-based analysis determined that pressure measurement and a simple phase-shifting algorithm with an appropriately chosen control phase is sufficient for suppression of oscillations, given enough control authority ([11, 7, 14, 6, 8, 3, 4]). Model based analysis determined that minimum information needed to calculate the best control phase requires estimation of parameters, including transport delay (or at least the corresponding phase shift), that are hard to obtain from pressure measurements alone [8, 3, 4]. Even if this difficulty could be circumvented, the sensitivity to modeling errors was likely to be high.

Need for developing an algorithm that would allow finding the best phase with minimum amount of a priori information that would work over large range of operating conditions and with minimum model assumptions seemed apparent. The operating conditions include fast engine acceleration and deceleration transients.

An experiment with active control of pressure oscillations in an industrial combustor has been conducted on 179MW and 230MW gas turbines by Siemens [16]. The pilot fuel has been modulated using a phase-shifting mechanism. The best control algorithm parameters were found manually at each operating condition. However, problems developed when the conditions were changing suddenly. Here is a quote from the paper by Siemens engineers and they coworkers describing experiments with Active Instability Control on 170MW engine:

"Further investigations of the effects of AIC showed de-

pendence of the required control parameters (gain and phase shift) on the operating conditions of the gas turbine (e.g., power level, pilot gas fraction). AIC operating parameters wich result in a clear reduction of oscillations for certain gas turbine operating conditions can cause a significant loss in performance of the control system during other gas turbine operating conditions. In the worst case, the heat release rate modulation induced by the controller can be in phase with the one resulting from the self-excitation, which results in a positive feedback and further amplification of the undesired oscillations. Therefore, the control parameters must be adjusted to the operating conditions quickly. Since the control parameters were set manually, difficulties arose when the operating conditions were subject to sudden changes. Therefore, an adaptive control algorithm is being developed, which seeks the optimum settings for gain and phase shift." [16].

The lack of a control algorithm that would allow for the search of control parameters automatically and would not magnify the pressure oscillations in the process of tuning was perceived by Siemens engineers to be the major obstacle in implementing Active Instability Control to suppress pressure oscillation on an industrial gas turbine.

The algorithm presented in this paper allows fast automatic tuning of control parameters and (under reasonable assumptions) can be guaranteed not to amplify the oscillations. Two extremum-seeking algorithms [17] were selected for tuning of the control phase. There was a technical challenge in finding a phase shifting mechanism that works for pressure oscillations varying over large frequency range and reliable pressure magnitude detection mechanism. This challenge has been overcome with a frequency tracking observer algorithm (based on Extended Kalman Filter described in [12]) that allows for fast and reliable estimation of the in-phase and quadrature components of the bulk pressure mode over large range of frequencies.

Performance specifications for extremum-seeking algorithms have been defined for algorithm initialization transients and engine acceleration transients. When initialized with a phase corresponding to amplification of oscillations, the algorithms should quickly produce and maintain phases corresponding to suppression of the oscillations. In the engine acceleration transients the algorithms should be able to suppress oscillations relative to uncontrolled levels.

The algorithms were tested on a single nozzle combustion rig at United Technologies Reserach Center in August 1998. More details on frequency tracking and classical extremum-seeking algortithm are included in [5]. The paper [18] provides more details on the triangular search extremum-seeking algorithm.

## 2 Adaptive algorithm description

### 2.1 Control architecture

The model analysis indicates that the combustion process can be modeled by a feedback interconnection of a second order lightly damped system representing an acoustic mode,

and a large delay followed by a saturated nonlinear function representing the heat release process [15] [13]. If the phase shift due to the heat release delay provides a positive feedback, then the damping of the system will be reduced and possibly achieve a negative value. In the latter case the system dynamics can settle on a limit cycle. One can easily show that phase-shifting control is an effective way of reducing the magnitude of the limit cycle. The phase shift can be implemented in many ways, including introducing a delay in control, using phase lead or lag, using LQG control, and self-tuned LMS algorithms. For our purpose phase-shifting using an observer was selected. The observer-based phase shifting control has several advantages: it is conceptually simple and its digital implementation requires less CPU time and offers better phase resolution that the delay algorithm. However, the most important feature of the observer based phase-shifting controller is its suitability for tuning. Firstly, the controller phase-shift is directly available for tuning. Secondly, an estimate of the magnitude of the pressure oscillations is readily available from the observer states. Hence, an extremum-seeking algorithm to tune the controller phase to reduce pressure magnitude can be implemented.

There was a technical challenge in finding an adaptive observer that works for pressure oscillations varying over large frequency range and reliable pressure magnitude detection mechanism. This challenge has been overcome with a frequency tracking observer algorithm based on Extended Kalman Filter described in [12] that allows for fast and reliable estimation of the in-phase and quadrature components of the bulk pressure mode over large range of frequencies. An extremum-seeking algorithm has been selected for tuning of the control phase. One of the reasons for choosing extremum-seeking for tuning the phase is that it is possible to guarantee convergence of the control parameters to the optimal value and stability of the overall system [9, 10].

Figure 1 shows the structure of the control algorithm. The control gain was fixed and only the control phase has been updated. Two distinct extremum-seeking algorithms were used. The first one described in more details in this paper relied on estimation of derivative of the pressure magnitude with respect to control phase by introducing a small sinusoidal variation in the control phase and measuring the response of the pressure magnitude at the corresponding frequency. The mean control phase was incremented by amount proportional to the estimated derivative. This algorithm will be referred to as a classical extremum-seeking algorithm. The other algorithm, described in [18], called the triangular search algorithm, used three past sampled average magnitude values to determine the new control phase. The idea behind this algorithm was to first find an interval that contains the extremum of a function and reduce the size of this interval at an exponential rate.

### 2.2 Frequency Tracking Observer Design

Observer based phase-shifting control algorithm that can work during engine acceleration and deceleration transients
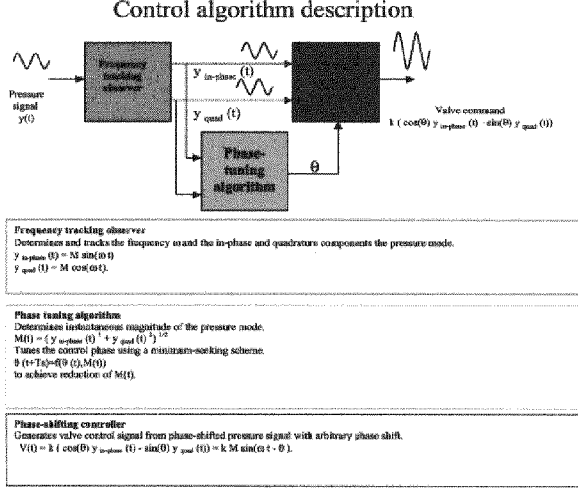
## Control algorithm description



**Frequency tracking observer**
Determines and tracks the frequency ω and the in-phase and quadrature components the pressure mode.
$y_{\text{in-phase}}(t) = M \sin(\omega t)$
$y_{\text{quad}}(t) = M \cos(\omega t)$.

**Phase tuning algorithm**
Determines instantaneous magnitude of the pressure mode.
$M(t) = (y_{\text{in-phase}}(t)^2 + y_{\text{quad}}(t)^2)^{1/2}$
Tunes the control phase using a minimum-seeking scheme.
$\theta(t+Ts)=f(\theta(t),M(t))$
to achieve reduction of $M(t)$.

**Phase-shifting controller**
Generates valve control signal from phase-shifted pressure signal with arbitrary phase shift.
$V(t) = k(\cos(\theta) y_{\text{in-phase}}(t) - \sin(\theta) y_{\text{quad}}(t)) = k M \sin(\omega t - \theta)$.

Figure 1: Adaptive algorithm for control of harmonic oscillations

requires a frequency tracking algorithm. A generalized version of a frequency tracking algorithm based on an Extended Kalman Filter studied in [12] has been implemented. Below we describe a digital version of the algorithm.

Consider a problem of estimation of in-phase and quadrature components of a sinusoidal signal $y(t) = M \sin(2\pi ft)$ with unknown frequency $f$, sampled at sample time $T_s$ from a noisy measurement. Th idea used in [12] was to represent the measurements $y(k) = M \sin(2\pi fkT_s)$ as the output of a nonlinear discrete-time system with the unknown constant frequency being one of the states.

$$x_c(k+1) = \cos(w(k))x_c(k) - \sin(w(k))x_s(k) \quad (1)$$
$$x_s(k+1) = \sin(w(k))x_c(k) + \cos(w(k))x_s(k) \quad (2)$$
$$w(k+1) = w(k). \quad (3)$$

The corresponding output equation is

$$y(k) = x_s(k). \quad (4)$$

Given measurements $y(k) = M \sin(2\pi fkT_s)$, under certain conditions one can estimate the unknown frequency $f$ (from the formula $f = \frac{w(k)}{2\pi T_s}$), and the in-phase and quadrature components of the signal $x_s(k)$, $x_c(k)$ using an observer.

We constructed an estimator for the nonlinear model (1)-(3) using an Extended Kalman Filter, i.e., a Kalman Filter designed for the linearization of the model about the current estimate (see [1]). In general, an Extended Kalman Filter algorithm estimates state x(k) of the nonlinear discrete-time system

$$x(k+1) = f(x(k)) + v_1(k) \quad (5)$$

from the measurement

$$y(k) = h(x(k)) + v_2(k). \quad (6)$$

$v_1(k)$, $v_2(k)$ are assumed to be Gaussian, independent, white noise signals, with zero means, and covariance matrices $Q$, $R$, respectively.

The Extended Kalman Filter (to be sometimes abbreviated to EKF) uses the measurement $y(k)$ to update the estimate of the state. The filter state is denoted $\hat{x}(k)$ and the state estimate error covariance matrix is denoted $P_s(k)$. The filter states are initialized at zero except for the frequency estimate.

Extended Kalman Filter update equations are:

given: previous filter state $\hat{x}(k-1)$, state estimate error covariance matrix $P_s(k-1)$, measured signal $y(k)$.

1. $K(k) = P_s(k-1)H(k-1)' * (H(k-1)P_s(k-1)H(k-1)' + R)^{-1}$ calculate update gain

2. $y_d(k) = y(k) - h(\hat{x}(k-1))$ filter output prediction error

3. $x_m(k) = \hat{x}(k-1) + K(k)y_d(k)$ state estimate using prediction error

4. $H(k) = \frac{\partial h}{\partial x}$, at $x = \hat{x}(k-1)$ linearization of output function

5. $F(k) = \frac{\partial f}{\partial x}$, at $x = x_m(k)$ linearization of vector field $f$

6. $P_m(k) = (I - K(k)H(k))P_s(k-1)$ state estimate error covariance update

7. $\hat{x}(k) = f(x_m(k))$ state prediction

8. $P_s(k) = F(k)P_m(k)F(k)' + Q$ state estimate error covariance prediction

We assume $R = 1$ and $Q = diag(q_1, \ldots, q_n)$. The choice of weights $q_i$ is the main tuning mechanism for the EKF. While they were introduced in the formulation of the filtering problem was as the variances to the state noise terms they can be thought of as tuning knobs for the filter.

A modified and extended version of the algorithm from [12] has been implemented in a digital control system on a DSP board to provide a frequency tracking and phase-shifting mechanism for control of combustion instability. Several extensions of model (1-2) were implemented. The most complex one has 8 states and involves modeling of first two harmonics of the bulk pressure mode, its unknown frequency, DC (low frequency) component, and longitudinal acoustic (750Hz) mode component.

Figures 2 and 3 illustrate performance of the frequency tracking Extended Kalman Filter. An 8-second long data record has been constructed off-line by concatenating four 2-

second long time traces of a pressure signal obtained during control experiment on United Technologies Research Center test rig. The four data points correspond to four different control phases. Figure 2 shows that the frequency estimate from the EKF algorithm agrees well the one obtained with a short-time PSD analysis. From Figure 3 we see that the EKF output traces the pressure signal very well.
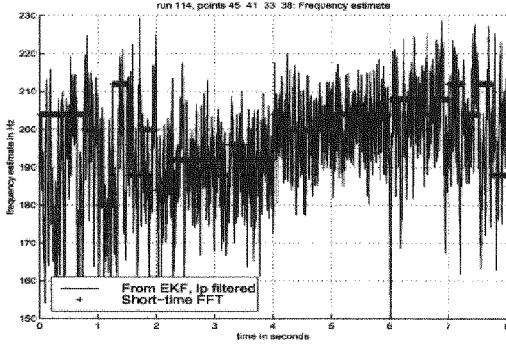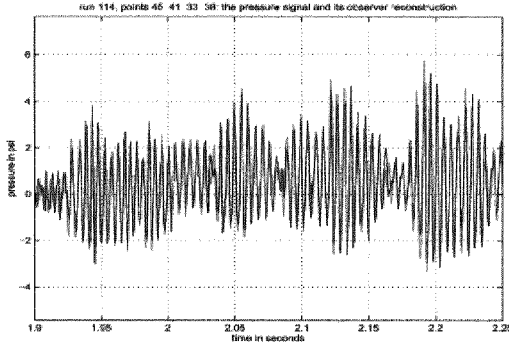


Figure 2: Frequency estimate from EKF and short-time PSD



Figure 3: Pressure signal and its reconstruction with EKF

Figures 4 to 9 show frequency tracking with Extended Kalman Filter when the combustor in the sector rig was warming up. Figures 4 to 6 show the on-line frequency estimate from EKF and short-time PSD. The frequency of the bulk acoustic mode increases because the speed of sound increases with temperature. Note that the frequency tracking algorithm was tracking the maximum frequency of the bulk pressure mode. The frequency estimate from EKF algorithm was smoother than the one shown in the previous section because the estimate from EKF was smoothen with an additional low-pass filter. Figures 7 to 9 show pressure signal and on-line estimates of the in-phase component of the pressure signal reconstructed with EKF. From comparison of FFTs one can see the band-pass filtering properties of the EKF. The in-phase and quadrature components of the bulk pressure mode have spectral content around 200Hz and thus the phase-shifted control signal would not be contaminated with other frequencies.

Figures 4 to 9 illustrate how fast the pressure oscillations frequency and magnitude can increase when the combustor operating conditions change. Figure 4 alone shows increase of frequency of pressure oscillation by $30Hz$ in 9 seconds. Overall, in less than 2 minutes the frequency of oscillations changed from about 150Hz to around 230Hz and its magnitude increased by a factor of 3. Changes in the frequency and magnitude of acoustic oscillations during an engine acceleration or deceleration could be even faster and more dramatic. It is very unlikely that a robust controller could cope with such conditions. The need for controller phase and gain scheduling with operating conditions is clear. Since for the lack of models the model-based scheduling of controller parameters is impossible, scheduling of controller parameters using an adaptive algorithm remains the only option.

## 2.3  Controller phase tuning using classical extremum-seeking algorithm

The classic algorithm for finding control phase $\theta$ such that the pressure magnitude achieves a local minimum at $\theta^*$ relies on introducing a sinusoidal variation into the control parameter $\theta$. Namely, at time $t$ the control parameter is given by

$$\theta(t) = \theta_m(t) + \theta_1 \sin(\omega t). \tag{7}$$

$\theta_m(t)$ is the mean value of the control parameter that is adjusted using an update equation that is described later. $\theta_1$ is the control parameter variation magnitude, usually chosen to be small. If the frequency $\omega$ is small enough, the magnitude $x_0(t)$ approximately follows the value of $x_0$ corresponding to the magnitude of the limit cycle corresponding to the control phase, so that the measured magnitude is

$$A(t) \approx g(\theta_m(t) + \theta_1 \sin(\omega t)) + \nu(t), \tag{8}$$

where $\nu(t)$ is a random component of the pressure magnitude that models disturbances driving the combustion process, and $g(.)$ is the function representing the dependence of the magnitude of the limit cycle corresponding on the control phase. Assuming that $\theta_1$ is small, one can approximate $A(t)$ as

$$A(t) \approx g(\theta_m(t)) + \frac{dg}{d\theta}(\theta_m(t))\theta_1 \sin(\omega t) + \nu(t). \tag{9}$$

An observer has been used to extract the components of the magnitude estimate of $A(t)$ at the frequency $\omega$. The observer has been constructed assuming that $A(t)$ is composed of a constant component and a harmonic component at the frequency $\omega$, i.e., the magnitude estimate $A(t)$ is an output of a linear system with three states, one modeling the constant component, and two modeling in-phase and quadrature components of a harmonic oscillator with the frequency $\omega$. The observer equations were

$$\dot{x}_1(t) = -\omega x_2(t) + l_1(A(t) - A_o(t)) \tag{10}$$
$$\dot{x}_2(t) = \omega x_1(t) + l_2(A(t) - A_o(t)) \tag{11}$$
$$\dot{x}_3(t) = l_3(A(t) - A_o(t)) \tag{12}$$
$$A_o(t) = x_2(t) + x_3(t). \tag{13}$$

with the gains $l_1$, $l_2$, $l_3$ chosen so that the observer error dynamics is stable. (In fact, a discrete-time version of this observer was implemented). Now, assuming that the observer gains are properly chosen, one can assume that after some transient the observer states are approximately

$$x_1(t) \approx \frac{dg}{d\theta}(\theta_m(t))\theta_1 \cos(\omega t) \qquad (14)$$

$$x_2(t) \approx \frac{dg}{d\theta}(\theta_m(t))\theta_1 \sin(\omega t) \qquad (15)$$

$$x_3(t) \approx g(\theta_m(t)). \qquad (16)$$

Now, an estimate of $\frac{dg}{d\theta}(\theta_m(t))$ can be obtained by the following demodulation of observer states:

$$z(t) := x_2(t)\sin(\omega t) + x_1(t)\cos(\omega t) \approx \frac{dg}{d\theta}(\theta_m(t))\theta_1. \qquad (17)$$

The control parameter equation will take form

$$\dot{\theta}_m(t) = -\sigma z(t), \qquad (18)$$

The parameters to choose are: the control parameter variation frequency $\omega$, the observer gains $l_1$, $l_2$, $l_3$, and the update gain $-\sigma$.

## 2.4 Controller phase tuning using triangular search algorithm

The triangular search algorithm is a self-exciting scheme. No external probing is required to find the direction of search. The purpose of the contraction coefficient is to gradually decrease the level of excitation when the control phase $\theta$ is close to the optimizing point. In a noise free and time invariant environment, this is to guarantee convergence with no residual error such as the case of a region of attraction. However, when noise is present and the plant is time varying, the excitation level must be kept at a sufficiently large level for all time in order to extract the correct information about the direction along which to move the control input. More details on the algorithm are presented in [18].

## 3 Experimental Results

In this section we present results of experiments in United Technologies Research Center conducted on 4 MW Single Nozzle Rig in August 1998 using full-scale engine fuel nozzle at realistic operating conditions. About 10% of the net fuel was modulated for control purposes using linear proportional valve. (For more details on the UTRC experiments see [6] and [8]. )

Performance specifications for the adaptive algorithm have been defined for algorithm initialization transients and engine acceleration transients. When initialized with a phase corresponding to amplification of oscillations, the algorithms should quickly produce and maintain phases corresponding to suppression of the oscillations. During the engine acceleration transients the algorithms should be able to suppress oscillations relative to uncontrolled levels.

To test the transient performance of the adaptive algorithm initialization transients have been introduced. The initial control phase varied significantly from the optimal one. The algorithms behaved very well at higher power condition (small pressure oscillations and medium level of broad-band disturbance) and reasonably well at lower power conditions (large pressure oscillations and large level of broad-band disturbance). Once reaching a neighborhood of the optimal value, the control phase usually stayed in a reasonably small neighborhood of that value, rarely produced control phases corresponding to level higher than uncontrolled levels, and always provided better average pressure oscillations levels than uncontrolled levels.

The triangular search algorithm tracked the minimum value well in a transient from higher power to lower power condition. This was a slow transient but the frequency changed by about 40Hz and the pressure magnitude and noise levels were changing dramatically. Classical algorithm with a fixed gain did not work during the transients, as the controller gain that was optimal at the higher power level was destabilizing the system at the lower power level. Gain adaptation would be needed for the classical algorithm to work at both power levels. The frequency and magnitude tracking mechanism worked very well during the transients.

The dependence of the mean pressure magnitude and frequency of the corresponding mode on the control phase has been determined experimentally at two power conditions, so that the optimal control phase was known a priori. This information allowed to check performance of the extremum-seeking algorithms. Initialization transients have been introduced, where the initial control phase varied significantly from the optimal one. Figures 10 to 31 show typical time histories of control phase and pressure magnitude (instantaneous and mean) estimate at two power conditions. The open-loop and optimal levels of the pressure as well as the optimal control phase are indicated by horizontal lines in the corresponding plots. oscillations

The experimental results are presented in Appendix.

For more details on experiments we refer to [5]. In general both phase tuning algorithms behaved very well at higher power condition (medium noise and small pressure oscillatios) and reasonably well at lower power conditions (large noise and pressure oscillations). Once reaching a neighborhood of the optimal value, the control phase usually stayed in a reasonably small neighborhood of that value, rarely produced control phases corresponding to level higher than uncontrolled levels, and always provided better average pressure oscillations levels than uncontrolled levels.

It has been concluded that the major factor affecting the performance of the extremum-seeking schemes is the "noise" present in the pressure magnitude. More precisely, the main trouble with implementation of extremum-seeking algorithm is that the pressure oscillations do not have a consistent instantaneous magnitude. In fact, the magnitude varies wildly. However, changing the control phase affects the mean value of the pressure and after some averaging time it is possible to determine the mean pressure magnitude as a function of

control phase with one minimum and one maximum (modulo 360 degrees). The fluctuating component of the pressure magnitude for a fixed phase is what we call noise. The noise can be attributed to an efect of turbulent flow in the combustor on the acoustic mode either directly, or via chemical reaction.

Since magnitude of the noise is a crucial factor that determines performance of the tuning mechanism, it is necessary to include a representative noise model in the engine dynamics model, if the latter is used to study performance of the tuning algorithms.

### 3.1 Simulated engine acceleration transient

A nominal gas turbine engine transient from 50% to 100% power conditions lasts a fraction of a minute. The changes in operating conditions appearing during engine acceleration and deceleration are likely to resemble the transients between different power levels on the single nozzle rig. Engine transient lasting fraction of a minute could not be simulated in experiments on the single nozzle rig. Instead, we tested the extremum-seeking algorithms in a simulated engine 30-second transient, where the measured magnitude versus control phase functions and lower and higher power were interpolated.

To simulate the transients the form of the averaged pressure magnitude model was assumed in accordance with the predictions of analysis of the physics-based reduced order model and the unknown parameters of the averaged model were determined from experiments (experiments are described in [5]). The identified model was

$$\dot{x}_0(t) = -\alpha(\theta(t))(x_0(t) - g(\theta(t))) \quad (19)$$

$$A(t) = x_0(t) + \nu(t), \quad (20)$$

where $\theta(t)$ is the controller phase, $x_0(t)$ is the mean pressure magnitude, $A(t)$ is the instantaneous pressure magnitude, and $\nu(t)$ is a random noise. The functions $g(.)$, $\alpha(.)$, and the statistics of (colored) noise $\nu(t)$ were identified from experiment. To simplify analysis we do not include the frequency tracking algorithm in the model. This is justified under the assumption that the frequency changes faster than the magnitude and that the frequency tracking algorithm is fast and stable. In other words, we assume that the frequency dynamics and the tracking algorithm contribute to the fast stable dynamics whose time scale is separated from the slow magnitude dynamics.

The triangular search algorithm performed well in the simulated transient (see Figure 11). It was determined that in order to work in a simulated transient from lower to higher power conditions, the classical algorithm would have to be modified to allow for adaptive gain change (by a factor of five). One fixed gain would not work at both power conditions.

Ability of an extremum-seeking algorithm to track the fast changing optimal control phase shift during the engine acceleration and deceleration transient conditions in the present of disturbance driving the system has been demonstrated in a simulation. However, there is need to study stability, robustness, and performance of the algorithms using analytical tools. Traditional methods based on time-scale separation are not sufficient as the time scale of of change of operating conditions is not well separated from the time scale of the transients in the dynamics. Preliminary analysis of performance limiations of extremum-seeking algorithms that does not expoits time-scale separation has been presented in [10].

## Conclusions

We presented results of experiments with two distinct extremum-seeking adaptive algorithms for control of combustion instability suitable for reduction of acoustic pressure oscillations in gas turbine over large range of operating conditions. The algorithms consists of a frequency tracking Extended Kalman Filter to determine the in-phase component, the quadrature component, and the magnitude of the acoustic mode of interest, and a phase shifting controller with the controller phase tuned using an extremum-seeking algorithms. The algorithms have been tested in combustion experiments involving full-scale engine hardware and during simulated fast engine transients.

## Acknowledgements

## References

[1] B.D.O. Anderson and J.B. Moore, *Optimal Filtering*, Prentice-Hall, Englewood Cliffs, New Jersey, 1979.

[2] A. Banaszuk, "A note on combustion instabilities," *UTRC Technical Report*, September 1997.

[3] A. Banaszuk, C. A. Jacobson, A. I. Khibnik, P. G. Mehta, "Linear and nonlinear analysis of controlled combustion processes. Part I: Linear analysis," *Proc. of the IEEE Conf. on Control Applications*, Kohala-Coast, Hawai, pp. 199–205, Aug. 1999.

[4] A. Banaszuk, C. A. Jacobson, A. I. Khibnik, P. G. Mehta, "Linear and nonlinear analysis of controlled combustion processes. Part II: Nonlinear analysis," *Proc. of the IEEE Conf. on Control Applications*, Kohala-Coast, Hawai, pp. 206–212, Aug. 1999.

[5] A. Banaszuk, K. Aryiur, M. Krstic, C. A. Jacobson, "An Adaptive Algorithm for Control of Combustion Instability," *submitted to Automatica*, 2000.

[6] J. M. Cohen, N. M. Rey, C. A. Jacobson, T. J. Anderson, "Active control of combustion instability in a liquid-fueled low-$NO_x$ combustor," *ASME/IGTI Gas turbine Expo and Congress*, Stockholm, Sweden, June 1998.

[7] J. P. Hathout, A. M. Annaswamy, M. Fleifil, A. F. Ghoniem, "A model-based active control design for thermoacoustic instability", *Combustion Sci. and Tech.*, vol. 132, pp. 99-105, 1998.

[8] J. R. Hibshman, J. M. Cohen, A. Banaszuk, T. J. Anderson, and H. A. Alholm, "Active control of combustion instability in a liquid-fueled combustor," *Proceedings of 1999 ASME Turbo Expo,* Indianapolis, 1999.

[9] M. Krstić and H. H. Wang, "Stability of extremum seeking feedback for general nonlinear dynamic systems," accepted for *Automatica*, 1998.

[10] M. Krstic, "Performance improvement and limitations in extremum seeking control," *System and Control Letters*, to appear.

[11] P. J. Langhorne, A. P. Dowling, N, Hooper, "Practical active control system for combustion oscillations," *Journal of Propulsion*, vol. 6, pp. 324-333, 1990.

[12] B. La Scala, "Approaches to Frequency Tracking and Vibration Control," *Ph.D. Thesis*, Dept. of Systems Engineering, The Australian National University, December 1994.

[13] R.M. Murray, C.A. Jacobson, R. Casas, A.I. Khibnik, C.R. Johnson Jr., R. Bitmead, A.A. Peracchio, and W.M. Proscia, "System Identification for Limit Cycling Systems: A Case Study for Combustion Instabilities," *Proceedings of 1998 American Control Conference*, Philadelphia, June 1997.

[14] Y. Neumeier, B. T. Zinn, "Active control of combustion instabilities using real-time identification of combustor modes", *Proc. of the IEEE Conf. on Control Applications*, Albany, NY, pp. 691-698, Sept. 1995.

[15] A. A. Peracchio and W. M. Proscia, "Nonlinear heat-release/acoustic model for thermoacoustic instability in lean premixed combustors," *ASME/IGTI Turbo Expo '98*, Stockholm, Sweden, June 1998.

[16] J.R. Seume, N. Vortmeyer, W. Krause, J. Hermann, C.-C. Hantschk, P. Zangl, S. Gleis, D. Vortmeyer, and A. Orthmann, "Application of Active Combustion Instability Control to a Heavy Duty Gas Turbine, ", *Proc. of ASME Asia '97 Congress and Exhibition*, Singapore, October 1997, ASME Paper 97-AA-119.

[17] J. Sternby, "Extremum control systems: An area for adaptive control?" Preprints of the *Joint American Control Conference*, San Francisco, CA, 1980, WA2-A.

[18] Y. Zhang, "Stability and Performance Tradeoff with Discrete Time Triangular Search Minimum Seeking", *Proc. of American Control Conference*, Chicago, June 2000.

# Appendix: experimental results with controller phase tuning using classical extremum-seeking algorithm
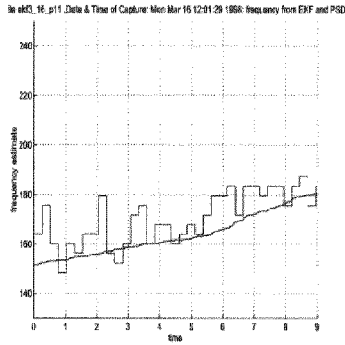
Figure 4: Frequency estimate from EKF and short-time PSD
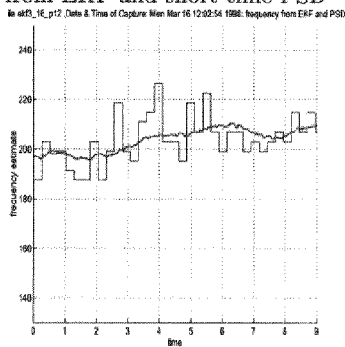


Figure 5: Frequency estimate from EKF and short-time PSD
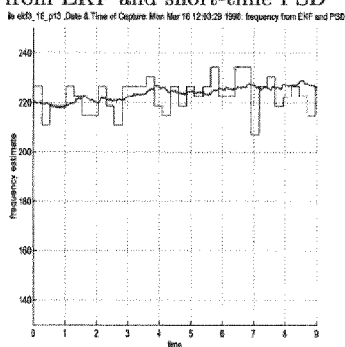


Figure 6: Frequency estimate from EKF and short-time PSD
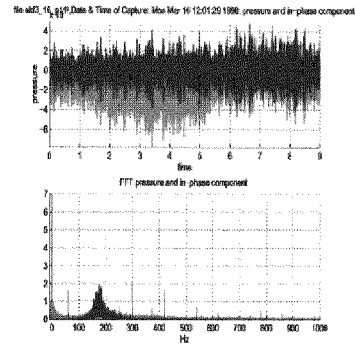


Figure 7: Pressure signal and its in-phase component recontracted with EKF: time traces and FFT
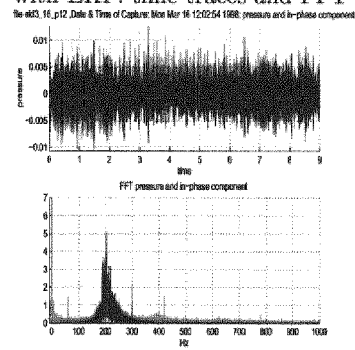


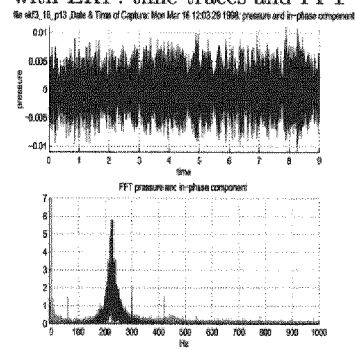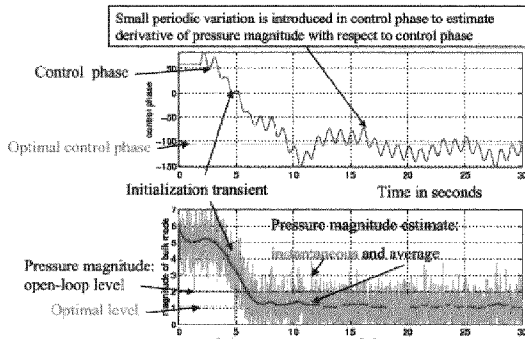Figure 8: Pressure signal and its in-phase component recontracted with EKF: time traces and FFT



Figure 9: Pressure signal and its in-phase component recontracted with EKF: time traces and FFT

Figure 10: Classical extremum-seeking algorithm. Typical initialization transient for higher power. Control phase and pressure magnitude as functions of time. Horizontal lines show optimal and close loop levels of mean pressure magnitude.
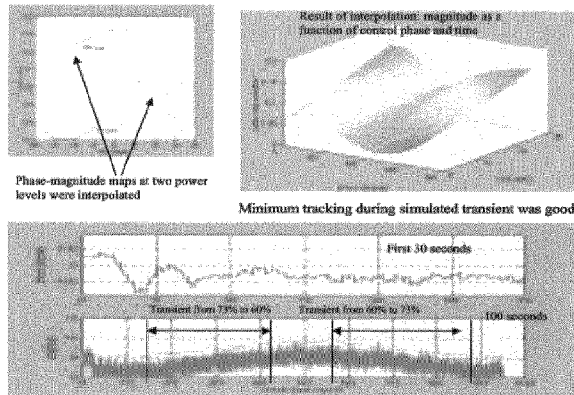


Figure 11: Perfomance of triangular extremum-seeking algorithm during a simulated engine transients
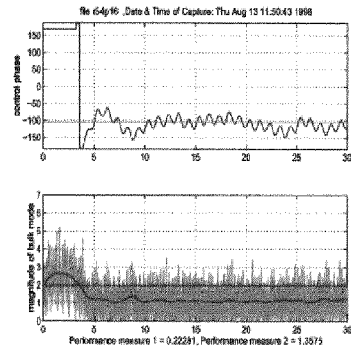


Figure 12: Controller phase tuning using classical algorithm. Initialization transient for higher power. $f = 1Hz$, $\theta_1 = 15$, $k = 1000$, $\theta_m(0) = 170$. Control phase and pressure magnitude as functions of time.
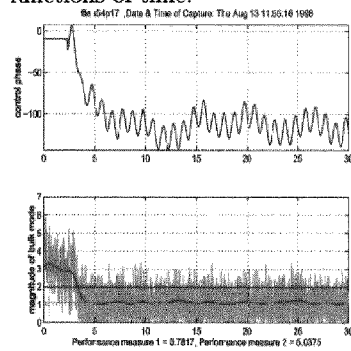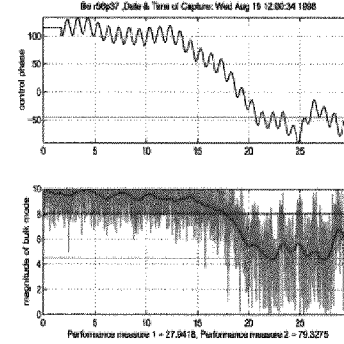


Figure 13: Controller phase tuning using classical algorithm. Initialization transient for higher power. $f = 1Hz$, $\theta_1 = 15$, $k = 1000$, $\theta_m(0) = -10$. Control phase and pressure magnitude as functions of time.
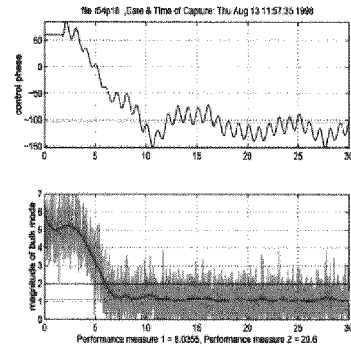


Figure 14: Controller phase tuning using classical algorithm. Initialization transient for higher power. $f = 1Hz$, $\theta_1 = 15$, $k = 1000$, $\theta_m(0) = 60$. Control phase and pressure magnitude as functions of time.
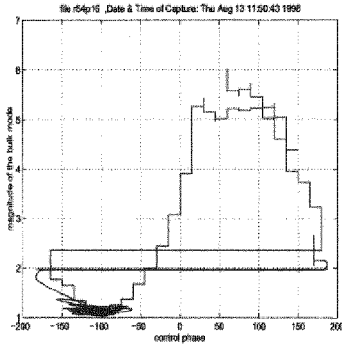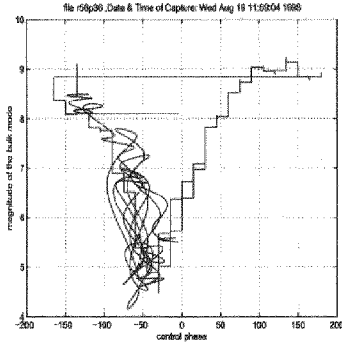
Figure 15: Controller phase tuning using classical algorithm. Initialization transient for higher power. $f = 1Hz$, $\theta_1 = 15$, $k = 1000$, $\theta_m(0) = 170$. Pressure magnitude as function of control phase.
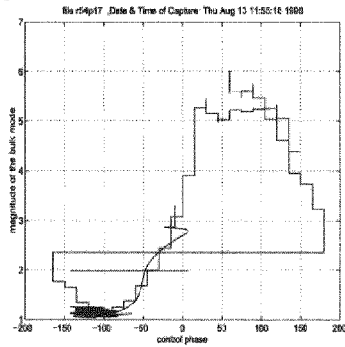


Figure 16: Controller phase tuning using classical algorithm. Initialization transient for higher power. $f = 1Hz$, $\theta_1 = 15$, $k = 1000$, $\theta_m(0) = -10$. Pressure magnitude as function of control phase.
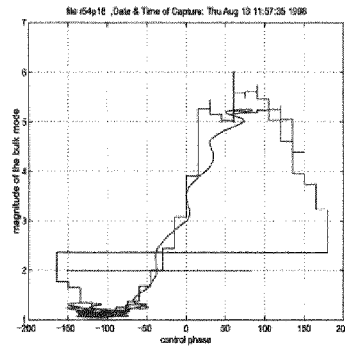


Figure 17: Controller phase tuning using classical algorithm. Initialization transient for higher power. $f = 1Hz$, $\theta_1 = 15$, $k = 1000$, $\theta_m(0) = 60$. Pressure magnitude as function of control phase.
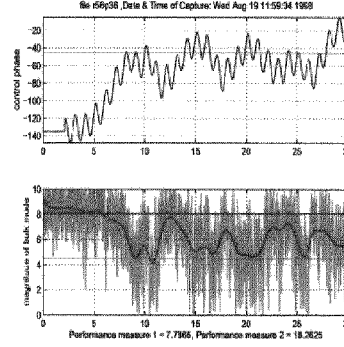


Figure 18: Controller phase tuning using classical algorithm. Initialization transient for lower power. $f = 1Hz$, $\theta_1 = 15$, $k = 150$, $\theta_m(0) = -135$. Control phase and pressure magnitude as functions of time.
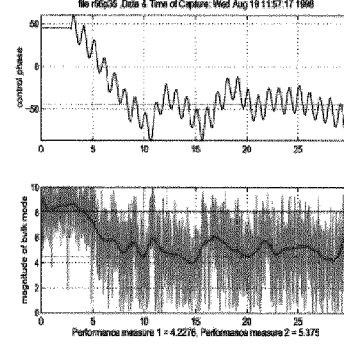


Figure 19: Controller phase tuning using classical algorithm. Initialization transient for lower power. $f = 1Hz$, $\theta_1 = 15$, $k = 150$, $\theta_m(0) = 45$. Control phase and pressure magnitude as functions of time.



Figure 20: Controller phase tuning using classical algorithm. Initialization transient for lower power. $f = 1Hz$, $\theta_1 = 15$, $k = 150$, $\theta_m(0) = 115$. Control phase and pressure magnitude as functions of time.

Figure 21: Controller phase tuning using classical algorithm. Initialization transient for lower power. $f = 1Hz$, $\theta_1 = 15$, $k = 150$, $\theta_m(0) = -135$ . Pressure magnitude as function of control phase.



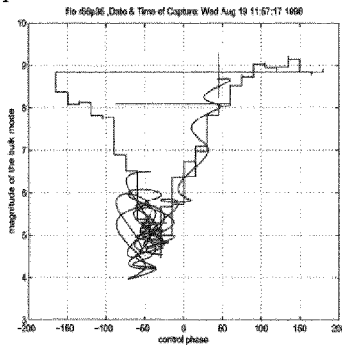Figure 22: Controller phase tuning using classical algorithm. Initialization transient for lower power. $f = 1Hz$, $\theta_1 = 15$, $k = 150$, $\theta_m(0) = 45$. Pressure magnitude as function of control phase.
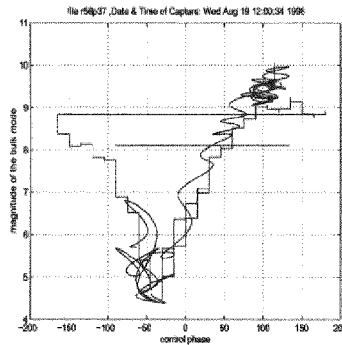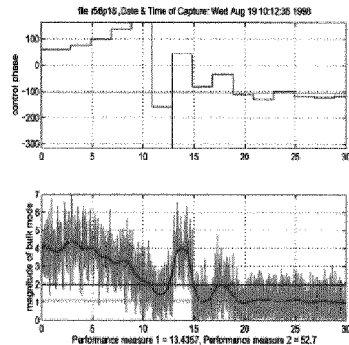


Figure 23: Controller phase tuning using classical algorithm. Initialization transient for lower power. $f = 1Hz$, $\theta_1 = 15$, $k = 150$, $\theta_m(0) = 115$. Pressure magnitude as function of control phase.



Figure 24: Controller phase tuning using triangular search algorithm. Initialization transient for higher power. $\theta_m(0) = 170$. Control phase and pressure magnitude as functions of time.
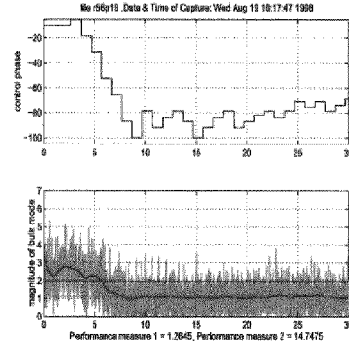


Figure 25: Controller phase tuning using triangular search algorithm. Initialization transient for higher power. $\theta_m(0) = -10$. Control phase and pressure magnitude as functions of time.
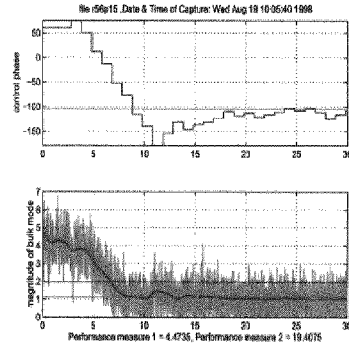


Figure 26: Controller phase tuning using triangular search algorithm. Initialization transient for higher power. $\theta_m(0) = 60$. Control phase and pressure magnitude as functions of time.
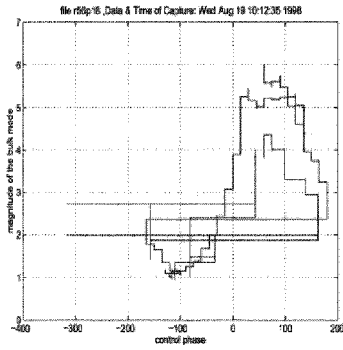
Figure 27: Controller phase tuning using triangular search algorithm. Initialization transient for higher power. $\theta_m(0) = 170$ . Pressure magnitude as function of control phase.
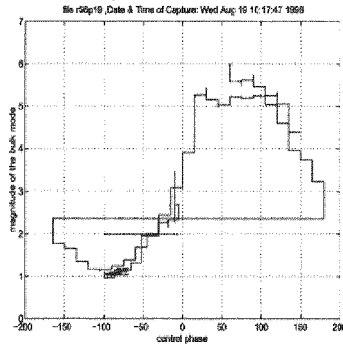


Figure 28: Controller phase tuning using triangular search algorithm. Initialization transient for higher power. $\theta_m(0) = -10$. Pressure magnitude as function of control phase.
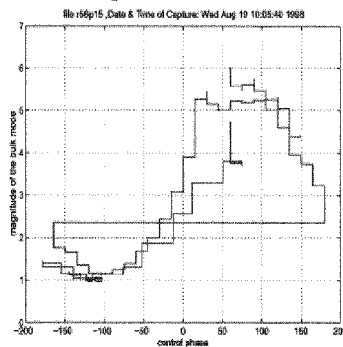


Figure 29: Controller phase tuning using triangular search algorithm. Initialization transient for higher power. $\theta_m(0) = 60$. Pressure magnitude as function of control phase.
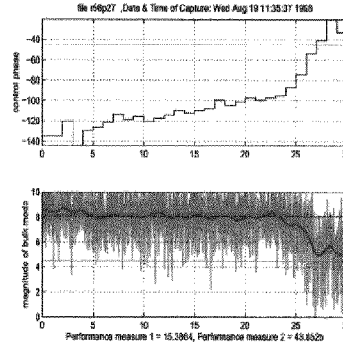


Figure 30: Controller phase tuning using triangular search algorithm. Initialization transient for lower power. $\theta_m(0) = -135$. Control phase and pressure magnitude as functions of time.
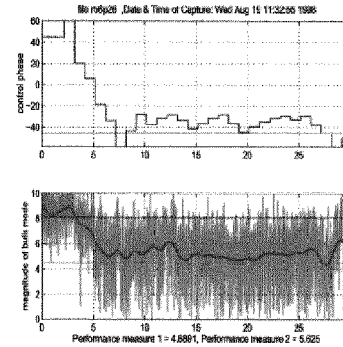


Figure 31: Controller phase tuning using triangular search algorithm. Initialization transient for lower power. $\theta_m(0) = 45$. Control phase and pressure magnitude as functions of time.
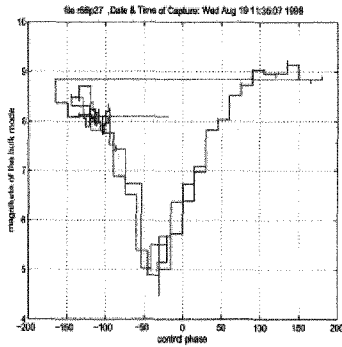
Figure 32: Controller phase tuning using triangular search algorithm. Initialization transient for lower power. . Pressure magnitude as function of control phase.
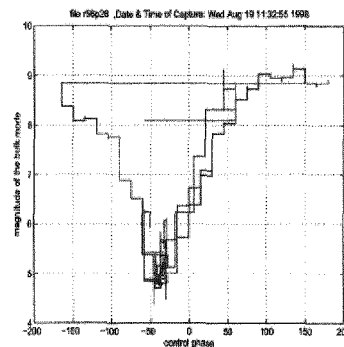


Figure 33: Controller phase tuning using triangular search algorithm. Initialization transient for lower power. $\theta_m(0) = 45$. Pressure magnitude as function of control phase.

## PAPER -31, A. Banaszuk

Question (F. E. C. Culick, USA)

Is there (i.e., can you give) a simple reason why your adaptive control algorithm(s) worked better for high power than for lower power conditions?

Reply

It appears that the high power condition was characterized by a linear model and the flat bottomed behavior of the phase-magnitude map was caused by peak-splitting (inability to improve performance beyond a certain point). We speculate that the "notchy" shape of the phase-magnitude function is caused by the system going in and out of a limit cycle. The limit cycling behavior was caused by a subcritical bifurcation. This increases sensitivity of the magnitude to the phase change around the minimum.

**This page has been deliberately left blank**

---

**Page intentionnellement blanche**